

## A MONTE CARLO SIMULATION OF MAGNETIC ORDERING IN ISING CUBIC FERROSPINELS

N. STANICA\*

*Institute of Physical Chemistry, Splaiul Independentei 202  
Bucharest 77208, Romania  
nstanica@icf.ro*

F. CIMPOESU

*Department of Applied Chemistry, University of Tokyo  
Tokyo, Bunkyo-ku 113-8656, Japan*

GIANINA DOBRESCU

*Institute of Physical Chemistry, Splaiul Independentei 202  
Bucharest 77208, Romania*

V. CHIHAIA

*GZG Crystallography, Göttingen University  
Goldschmidtstr. 1, Göttingen, Germany*

LUMINITA PATRON

*Institute of Physical Chemistry, Splaiul Independentei 202  
Bucharest 77208, Romania*

G. MUNTEANU

*Institute of Physical Chemistry, Splaiul Independentei 202  
Bucharest 77208, Romania*

C. G. BOSTAN

*Lightwave Devices Group, MESA Research Institute  
University of Twente, P. O. Box 217, 7500 AE  
Enschede, The Netherlands*

Received 1 December 2003

Accepted 16 March 2004

This work signifies the next step in our way in the magnetic properties simulation of spin clusters and extended networks containing quantum spins, by original FORTRAN codes

\*Corresponding author: nstanica@icf.ro

based on Heisenberg–Dirac–VanVleck (HDVV) or Ising approaches, using Full Diagonalization Heisenberg Matrix (FDHM) or Monte Carlo–Metropolis (MCM) procedure, respectively.

We present the results of magnetic Monte Carlo studies on a magnetite type lattice, Ising model ferrimagnet that provide insight into the exchange interactions involved in Cubic Ferros spinels. We have demonstrated that a comparatively simple model can reproduce ferrimagnetic behavior of ferros spinels, particularly for magnetite.

*Keywords:* Molecular magnets; ferrimagnets; cubic ferros spinels; Ising–Monte Carlo study.

## 1. Introduction

Strong magnetism was first discovered not in a metal but in magnetite, which is a main constituent of “lodestone”. Magnetite belongs to a very large class of non-conducting, strongly magnetic compounds whose magnetic properties qualitatively resemble those of ferromagnetic metals. These samples exhibit spontaneous magnetization,  $M_s$ , below a critical temperature,  $T_c$  and have domain structure.

However, there are significant quantitative differences. The paramagnetic susceptibility well above  $T_c$ , follows a Curie–Weiss law, with a negative Weiss constant,  $\theta$ , in contrast to the positive  $\theta$  characterizing a ferromagnetic metal.

In particular the  $M_s$  versus  $T$  curves show greater variability of shape than those of the ferromagnetic metals and alloys; many ferrimagnetics have  $M_s$  versus  $T$  curves with more complicated shapes, including the cases in which  $M_s$  falls sharply to zero at an intermediate temperature and immediately rises sharply again before decreasing finally to zero at  $T_c$ . The variability of shape, particularly the case of “compensation temperature” where  $M_s$  falls to zero and rises again, is characteristic of ferrimagnetism.

The behavior of the compensation point has important technological applications particularly in the field of thermomagnetic recording, since at this point, only a small driving field is required to change the resultant magnetization of the material.

These differences have been traced to the fact that the strongest interactions between magnetic ions in these materials are negative, rather than positive as in ferromagnetic metals, i.e. they favor antiparallel alignment of neighboring magnetic moments. As a result, the magnetic ordering in a crystal involves two or more interpenetrant sublattices that are spontaneously magnetized in different directions.

Following Néel’s suggestion,<sup>1</sup> the name ferrimagnetism is used to cover the behavior of materials in which the overall spontaneous magnetization is a resultant of two or more sublattice magnetizations of these kinds. Generally, it is the crystal structure of a ferrimagnetic compound that determines the detailed form of the ordering into magnetic sublattices. The two crystal types to which the most intensely investigated ferrimagnetics belong are those known as “spinel” and “garnets”, classes of materials currently finding important technical applications.

The general chemical formula for the compounds that may crystallize in the spinel structure is  $MQ_2X_4$ , where

- $X$  is a non-magnetic divalent ion which may be sulfur or selenium or, as in the large majority of studied cases, oxygen.

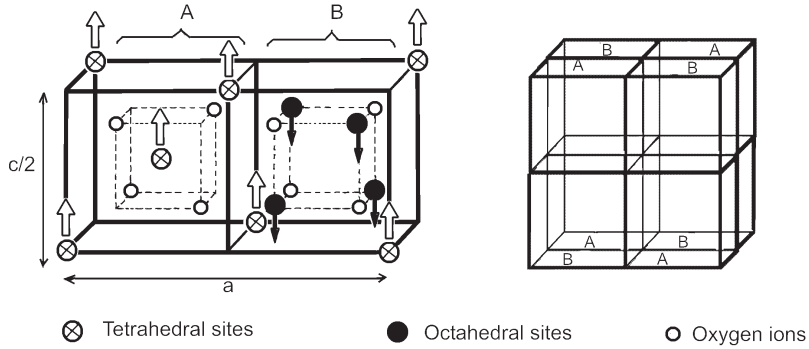


Fig. 1. Spinel structure; left — Two octants of the cubic elementary cell of a spinel structure (if cubic,  $c = a$ ); right — Full cubic elementary cell.

- $M$  is a divalent ion of a metal such as Mn, Fe, Ni, Co, Cu, Zn or Mg.
- $Q$  is a trivalent ion of a metal such as Mn, Fe, Co, Al or Ga.

$M$  and  $Q$  are the magnetic ions in a ferrimagnetic spinel. The spinel compounds containing iron, i.e.  $MFe_2O_4$ , are generally called ferrites and form a large group that includes the simple ferrimagnetic compound, magnetite  $Fe_3O_4$ . In these ferrites there are two oppositely directed sublattices each of these may contain both  $M$  and  $Q$  ions.

Considering the possibility of static disorder of the  $M$  and  $Q$  ions over the two types of coordination sites, there is a  $1/3$  ratio of metal ions with given spin orientation, while the remaining  $2/3$  adopt opposite alignment, see Fig. 1.

Figure 1 (left) shows the two octants of the cubic elementary cell of a spinel structure and the cation and anion sites in a primitive unit cell (if cubic,  $c = a$ ). Each of these octants is repeated in diagonally opposite corners of the Full Cubic Elementary Cell (see Fig. 1 right). The arrows indicate the Néel magnetic structure.

For more complex systems involving many sublattices or canted moments, the net spontaneous magnetization is not very informative and for detecting magnetic order on the sublattices are used other experimental or theoretical methods. For canted materials in particular, the application of a large enough magnetic field to align  $M_s$  against anisotropy can modify<sup>2</sup> the pattern of order.

The neutron diffraction<sup>3</sup> on a magnetite crystal supplied the first direct confirmation of Néel<sup>1</sup> hypothesis about interpenetrant, differently oriented magnetic sublattices. The neutron experiments have shown that, in fact there are several kinds of ferrimagnetic ordering involving canted spins, as well as the straightforward co-linear arrangements of the simple ferrites.

Magnetic measurement<sup>4-7</sup> of resultant spontaneous magnetizations for ferrimagnetic samples can yield only such information, if particular theoretical models<sup>8</sup> are used to separate the contributions and show the inadequacies of the molecular-field models.

In principle, the mean field approximation can be applied in the paramagnetic region and in the ordered phase; however, this method leads to a large overestimation of the ordering temperature.<sup>9</sup> The deviations of the specific heat obtained by mean field approaches comparatively with experimental values are closely associated with spontaneous sublattice magnetizations. They are due to the neglect of the energy associated with short-range order.

We demonstrate that besides neutron-diffraction method, a Ising–Monte Carlo simulation based on the Metropolis algorithm give the possibility to determine Néel (or Curie) temperature  $T_N(T_C)$ , the variation with temperature of spontaneous sublattice magnetizations, the specific magnetic heat and the magnetic susceptibility.

In this paper we present the results of Monte Carlo simulations of an Ising ferrimagnet on a magnetite type lattice. This work presents new advances in the simulation the magnetic properties of spin clusters<sup>10–12</sup> and extended networks containing quantum spins<sup>13–15</sup> by original FORTRAN codes based on Heisenberg–Dirac–VanVleck (HDVV) or Ising approaches, using Full Diagonalization Heisenberg Matrix (FDHM) or Monte Carlo (MC) procedure, respectively.

## 2. Methodology

The Ising Spin model was chosen for this study since it is known to show a transition to long-range order at a finite, non-zero temperature.<sup>16</sup>

Among the variety of approximate methods available in the literature, the Monte Carlo technique (MC), based on the Metropolis algorithm,<sup>17</sup> generates a sampling of states following the Boltzmann distribution that preferentially contains configurations which minimize interaction energy of the system and bring important contributions to the magnetization at temperature  $T$ .<sup>18</sup>

All the simulations were performed on finite samples, thus introducing systematic errors. To minimize these errors, the edge perturbation and accelerate convergence towards the infinite lattice limit, periodic boundary conditions (PBC) were adopted.<sup>19</sup>

To obtain reliable results, the optimal sizes of the samples were determined by carrying out simulations on a range of different sample sizes (Table 1). The minimum size that showed a finite-size effect for the studied reduced temperature range  $kT/|J_{ab}|$  was from only one Full Cubic Elementary Cell (FCEC, see Fig. 3).

Table 1. Samples sizes used in simulations.

Number of FCEC for Sample	Number of Octants for MC Analysis	Number of Octants for PBC Conditions	Number of Sites for MC Analysis	Number of Surface Sites/Number of Bulk Sites
1	8	56	24	7.00
8	64	152	192	2.40
27	216	296	648	1.40
64	512	488	1536	0.95

That means a sample of 64 octants from which 8 for MC analysis and 56 octants for PBC conditions.

Because the CPU time increases significantly with the size of the problem, for our first test of the algorithm we chose only 8 FCECs. For each site, at least  $10^4$  Monte Carlo Steps (MCS) were performed and first  $5 \cdot 10^3$  were discarded as the initial transient stage.<sup>19</sup> To avoid a freezing of the spin configuration,<sup>19</sup> we have used a low cooling rate according to the following equation:

$$(P_1)_{i+1} = 0.95^*(P_1)_i \quad (1)$$

where  $P_1 \equiv \frac{kT}{|J_{ab}|}$ , is reduced temperature parameter.

So a periodic boundary “magnetite lattice” with 192, 648 or 1536 sites was populated with two spin types (for inverse spinel, see Fig. 1),  $S_A^{1,2} = \frac{5}{2}$ ,  $S_B^{4,6} = \frac{5}{2} (\pm \frac{5}{2}, \pm \frac{3}{2}, \pm \frac{1}{2})$  and  $S_B^{3,5} = 2(\pm 2, \pm 1, 0)$  on separate sublattices,  $A$  and  $B$ . Initial spin states were randomly assigned.

The energy of each  $A$  site is described with the Hamiltonian:

$$E_i^A = g_i \mu_B H_z S_{zi}^A + D_i^A (S_{zi}^A)^2 - 2J_{ab} \sum_n S_i^A S_j^B - 2J_{aa} \sum_n S_{zi}^A S_{zj}^A \quad (2)$$

and for each  $B$  site with:

$$E_i^B = g_i \mu_B H_z S_{zi}^B + D_i^B (S_{zi}^B)^2 - 2J_{ab} \sum_n S_{zi}^B S_{zj}^A - 2J_{bb} \sum_n S_{zi}^B S_{zj}^B \quad (3)$$

where  $n$  indicates summation over the nearest neighbors from sublattices  $A$  or  $B$ .

$J_{ab}$  is the nearest neighbor exchange constant between the  $A$  and  $B$  spin sublattices and  $J_{aa}$  or  $J_{bb}$  indicates the nearest neighbor exchange constant between the sites within the same sublattice  $A$  or  $B$ , depending on the sublattice to which  $i$  belongs.

We have considered the case of cubic symmetry with only nearest-neighbour  $A$ - $B$  antiferromagnetic,  $A$ - $A$  and  $B$ - $B$  ferromagnetic interactions.

Néel model for ferros spinels, which has the cation spins on the tetrahedral ( $A$ ) interstices of the anion sublattice parallel to one another and antiparallel to all the cation spins on the octahedral ( $B$ ) interstices, is obviously correct if only a negative  $J_{ab}$  interaction exists. However, the introduction of “competing” interactions removes the simplicity of the problem.

The parameters  $J_{ab}$ ,  $J_{aa}$  or  $J_{bb}$  may be related to the Heisenberg theory, which assumes localized atomic moments coupled through exchange interactions that depend on the overlap of non-orthogonal, atomic orbitals of neighboring atoms.

In the present work,  $H_z$  is strength of an external magnetic field and  $D_i^{A,B}$  is the crystal field were fixed at zero. Even though it is possible to include them explicitly in MC Ising program (this kind of term could be necessary in order to take into account the noncollinear configurations), we avoided overparametrization effects.

For each Monte Carlo Step (MCS), one site is picked at random and the spin state changed. If this change results in a lower energy  $E_i$  the change is accepted automatically; if not, the change is accepted with the probability

$$p = e^{-\Delta E/kT} \quad (4)$$

where  $\Delta E$  is the energy difference between the new and the old spin states. Configurations were generated by randomly sweeping through the lattice and flipping the spins one at time according the heat-bath algorithm (to do one sweep means to visit randomly all the spins from the system, more precisely, to visit every spin at least once). The parameters  $J_{ab}$ ,  $J_{aa}$  or  $J_{bb}$  are substituted by the following reduced parameters,

$$P_1 \equiv \frac{kT}{|J_{ab}|}, \quad P_2 \equiv \frac{J_{aa}}{|J_{ab}|}, \quad P_3 \equiv \frac{J_{bb}}{|J_{ab}|}. \quad (5)$$

Mainly, we present the results of 121 runs for a sample with 8 FCEC. This means that  $P_2$  and  $P_3$  are fixed for each run at one of values from 0 to 1.0 by steps of 0.1 and for each of 121 runs,  $P_1$  is varied by Eq. (1) which gives the cooling rate.

The critical temperatures,  $T_{\text{crit}}$  or  $(P_1)_{\text{crit}} \equiv \left(\frac{kT}{|J_{ab}|}\right)_{\text{crit}}$ , were calculated by locating the maximum value of the specific heat.

Our program calculates the Internal Energy, the Specific Magnetic Heat, the Resultant and Sublattice Magnetizations, and the associated Susceptibilities by equations which are given everywhere.<sup>15</sup>

### 3. Results

As  $J_{aa}$  and  $J_{bb}$  increase there is a monotonic increase in  $T_N$ , reflecting the increasing total magnetic energy of the system. Variation of  $(P_1)_{\text{crit}} \equiv \frac{k(T)_{\text{crit}}}{|J_{ab}|}$  versus  $P_2 = \frac{J_{aa}}{|J_{ab}|}$  and  $P_3 = \frac{J_{bb}}{|J_{ab}|}$  is shown in Figs. 2 and 3. These results are confirmed<sup>20</sup> for layered, bimetallic ferrimagnets that show both compensate and non-compensate behavior at low temperatures. Figures 2 and 3 illustrate that the  $P_3$  parameter is critical in determination of the stable spin configuration and is experimentally confirmed<sup>4</sup> for various systems of ferrosphenels.

Below the Néel (Curie) temperature of a collinear ferrimagnet, there is a spontaneous magnetization, just as in the ferromagnets. However, in this case the magnetization is the vector sum of the magnetizations of the two antiparallel sublattices and therefore has magnitude

$$M_{S\text{-res}} = |M_{S\text{-}bb} - M_{S\text{-}aa}|. \quad (6)$$

Because the sublattice magnetizations have quite different temperature dependences, the  $M_s$  versus  $T$  curves are not restricted to a Brillouin-type shape, as in the case for ferromagnets (Fig. 4).

If only one sublattice is saturated (or close to the saturation) it is apparent that the interaction acting on the unsaturated paramagnetic ions is smaller than that acting on the saturated paramagnetic ions. Therefore the magnetization of the

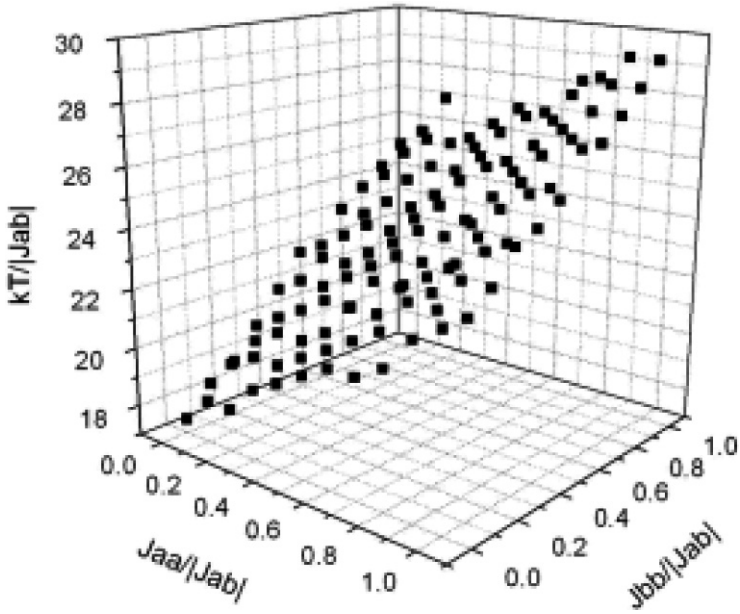


Fig. 2.  $\frac{kT}{|J_{ab}|}$  versus  $\frac{J_{aa}}{|J_{ab}|}$  and  $\frac{J_{bb}}{|J_{ab}|}$  ( $P_1$  versus  $P_2$  and  $P_3$ ).

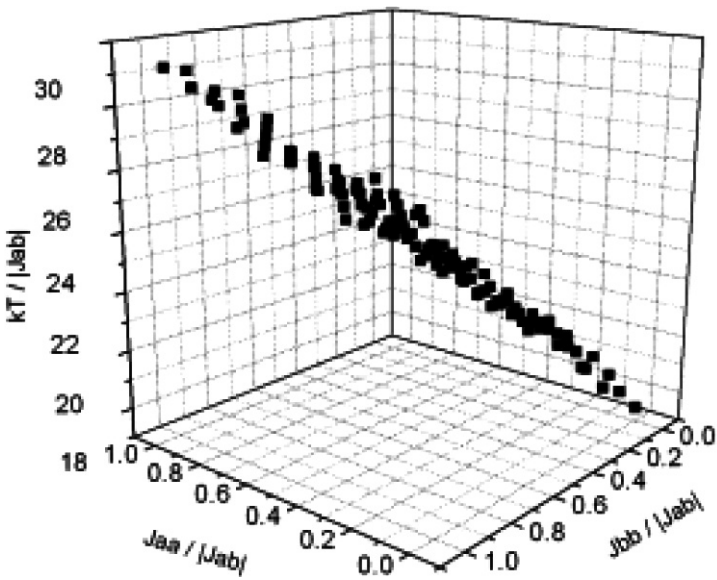


Fig. 3.  $\frac{kT}{|J_{ab}|}$  versus  $\frac{J_{aa}}{|J_{ab}|}$  and  $\frac{J_{bb}}{|J_{ab}|}$  ( $P_1$  versus  $P_2$  and  $P_3$ ).

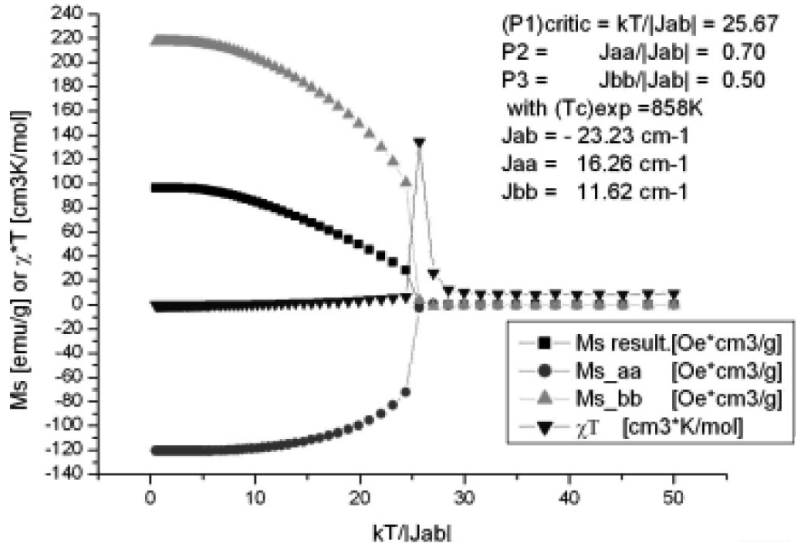


Fig. 4. Resultant spontaneous magnetization  $M_{S\_res.}$ , sublattice spontaneous magnetizations  $M_{S\_aa}$ ,  $M_{S\_bb}$  and, susceptibility\* temperature product versus reduced temperature parameter.

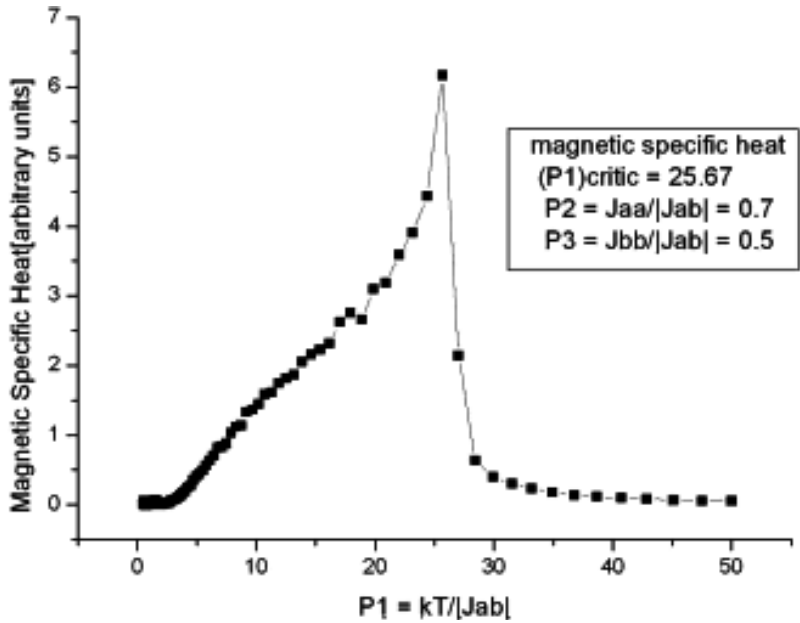


Fig. 5. Magnetic specific heat versus reduced temperature parameter.



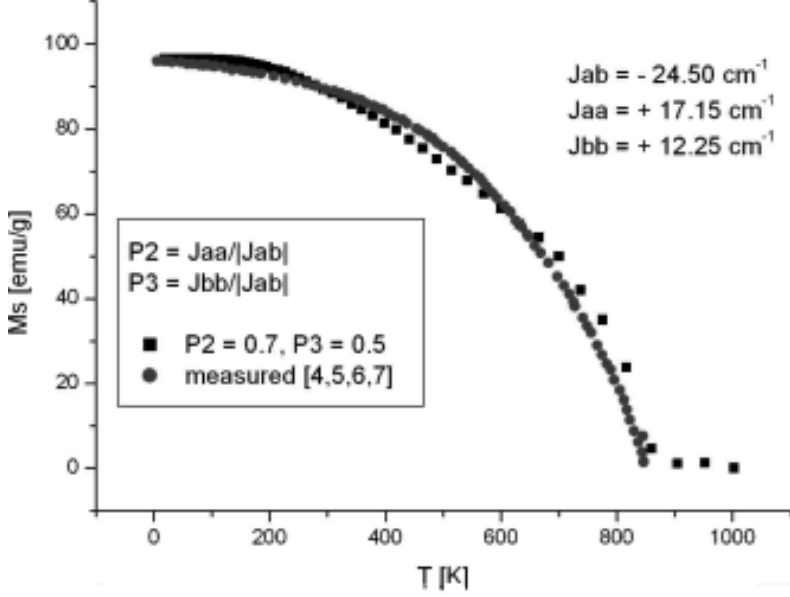


Fig. 6. The spontaneous measured (see Fig. 4 for Fe) and calculated magnetizations.

unsaturated sites decreases with  $T$  faster than that of the saturated sites, so  $M_{S\_res}$  decreases if it is parallel to the unsaturated sites.

As in the case of ferromagnets, there is a second-order transformation at the order  $\leftrightarrow$  disorder transition temperature that is marked by the anomalies in the magnetic susceptibility (Fig. 4) and specific heat (Fig. 5).

Because there is the entropy associated with the magnetic ordering, a magnetic contribution to the specific heat must be expected. Close to the Curie temperature, the rate of change of the long-range order, for which  $M_S$  is a measure, is high and a specific heat anomaly would be expected similar to those observed in ferromagnetic and antiferromagnetic crystals.

Taking  $J_{ab} = -24.50 \text{ cm}^{-1}$ ,  $J_{aa} = +17.15 \text{ cm}^{-1}$  and  $J_{bb} = +12.25 \text{ cm}^{-1}$ , the data shown in Fig. 6 are obtained; calculated and experimental results are presented for comparison. Clearly, the model is in agreement with the observed data.

By comparing measured<sup>4-7</sup> and calculated curves we obtained parameters  $P_1, P_2, P_3$  and consequently  $J_{ab}, J_{aa}$  and  $J_{bb}$ .

#### 4. Conclusions

We have demonstrated that a comparatively simple model can reproduce ferrimagnetic behavior of ferrosinels, particularly for magnetite.

Future improvements could be focused on the following points:

- (1) to upgrade the precision of the obtaining critical temperature corresponding to the maximum in specific magnetic heat,
  - (a) by improving the cooling rate from Eq. (1) (there are necessary more points for a more exact shape of specific heat peak, at least in vicinity of  $T_C$ );
  - (b) by using 27 or 64 FCEC, for a greater size of MC analyzed sample;
- (2) to use crystal field term, to take into account “noncollinear contributions”;
- (3) to use [5]  $g_{\text{eff}}^{\text{Fe}_3\text{O}_4} = 2.15$  (comparatively with  $g = 2$  used for us in this paper);
- (4) it will be necessary also to verify for magnetite, the  $T^{3/2}$  law, below<sup>21</sup> about 10 K.

## Acknowledgments

The authors N.S. and F.C. would like to acknowledge financial support from INTAS.

## References

1. Néel L, *Ann Phys* **12**(3):137, 1948.
2. Geller S, Remeika JP, Williams HJ, Espinosa GP, Sherwood RC, *Phys Rev* **137A**:1034, 1965.
3. Menyuk N, Dwight K, Wold A, *J Phys Radium* **25**:528, 1964.
4. Goodenough JB, *Magnetism and the Chemical Bond*, pp. 119, 127, 199, 1963.
5. Martin DH, *Magnetism in Solids*, pp. 41, 50, 241, 1967.
6. Smit J, Wijn HPJ, *Ferrites*, John Wiley & Sons, Inc., New York, 1959.
7. Pauthenet R, *Compt Rend* **230**:1842, 1950; *J Phys Radium* **12**:249, 1951; *Ann Phys* **7**:710, 1952.
8. Riste F, Tenzer L, *Phys Chem Solids* **19**:117, 1961.
9. Herpin A, *Théorie du magnétisme* I.N.S.T.N.:Saclay, 1968.
10. Stanica N, Ph. D. Thesis, Romanian Academy, Institute of Physical Chemistry, 1997.
11. Stanica N, Lepadatu C, Jitaru I, *Rev Roum Chim* **43**(5):433, 1998.
12. Stanica N, Stager CV, Cimpoesu M, Andruh M, *Polyhedron* **17**(10):1787, 1998.
13. Mihaiu S, Stanica N, Zaharescu M, *J Optoelectr Adv Mat* **3**(4):915, 2001.
14. Madalan AM, Roesky HW, Andruh M, Noltemeyer M, Stanica N, *Chem Commun* 1638, 2002.
15. Stanica N, Munteanu G, Carp O, Patron L, Bostan CG, *Rev Roum Chim* **47**(10–11):1217, 2002.
16. Onsager L, *Phys Rev* **65**:117, 1942.
17. Metropolis N, RosenBluth AW, RosenBluth MN, Teller AH, Teller E, *J Chem Phys* **21**:1087, 1953.
18. Boullant E, Cano J, Journaux Y, Decurtins S, Gross M, Pilkington M, *Inorg Chem* **40**:3900, 2001.
19. Binder K, Herman DW, *Monte Carlo Simulations in Statistical Physics. An Introduction*, 3rd ed., Springer, Berlin, 1997.
20. Carling SG, Day P, *Polyhedron* **20**:1525, 2001.
21. Meyer H, Harris AB, *J Appl Phys* **31**:Suppl., 330S, 1960.